A Novel Modified-T Equivalent Circuit for Modeling LTCC Embedded Inductors with a Large Bandwidth

T.S. Horng, J.M. Wu, L.Q. Yang, and S.T. Fang

Department of Electrical Engineering, National Sun Yat-Sen University, Kaohsiung, 804, Taiwan

Abstract — **In this paper, a modified-T equivalent-circuit model for three-dimensional (3-D) spiral inductors embedded in a multilayer low-temperature cofired ceramic (LTCC) is first presented to achieve a remarkably large bandwidth. This model combines a core circuit, a five-element modified-T model, to include the effects of transmission line with electrical length up to π, and several resonators to consider the effects due to coil coupling and finite ground plane. It is emphasized that most of the elements in this equivalent-circuit model can be extracted directly from the measured S parameters. Compared to the conventional Π-section model that is valid only up to the first self resonant frequency (SRF), this model includes more higher-order SRFs and results in several times larger bandwidth.**

I. Introduction

Spiral inductors can be viewed as passive interconnects that are conventionally modeled using Π- or T-section models [1]-[3]. Although several additional capacitances and resistances have been included to account for coupling and loss in coil and substrate, the model is still narrow-banded due to the nature of Π- and T-section models that cannot represent a transmission line over a wide frequency range effectively. The distributed model using multiple Π- or T-sections can be applied to overcome this drawback [4],[5]. However, it is difficult to find these distributed elements from the measured S parameters without an intensive optimization scheme. This is because the measured S parameters represent overall frequency response of distributed sections and lack useful information in segmentation for individual section. This paper breaks through the above-mentioned modeling barriers by inventing a five-element modified-T circuit that can approximate quite closely a lossless transmission line with electrical length up to π, the well-known period of transmission-line effects. In conjunction with several lossy resonators that account for coupling and loss in coil and substrate, this modified-T circuit can be expanded to model a real spiral inductor. As an example, in the following sections we will demonstrate an efficient modified-T modeling procedure for a 6.8 nH spiral inductor embedded in a multilayer LTCC substrate.

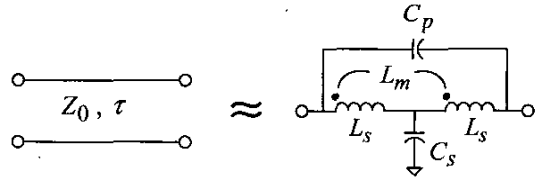

Fig. 1. A five-element modified-T equivalent circuit for modeling a lossless transmission with electrical length up to π.

II. Modified-T Model for Transmission Lines

For the lossless transmission line shown in the left of Fig. 1, its *Z* and *Y* network parameters are given as

$$Z_{11}^{TL} = Z_{22}^{TL} = -jZ_0 \cot\theta \tag{1}$$

$$Z_{12}^{TL} = Z_{21}^{TL} = -jZ_0 \csc\theta \tag{2}$$

$$Y_{11}^{TL} = Y_{22}^{TL} = -jY_0 \cot\theta \tag{3}$$

$$Y_{12}^{TL} = Y_{21}^{TL} = jY_0 \csc\theta \tag{4}$$

where $Y_0 = 1/Z_0$ and $\theta = \omega\tau$. For the five-element modified-T circuit shown in the right of Fig. 1, its *Z* and *Y* network parameters can be found as

$$Z_{11}^{MT} = Z_{22}^{MT} = \frac{(j\omega L_s + \frac{1}{j\omega C_s}) + j\omega C_p[-\omega^2(L_s^2 - L_m^2) + 2\frac{2(L_s + L_m)}{C_s}]}{1 - 2\omega^2 C_p(L_s + L_m)} \tag{5}$$

$$Z_{12}^{MT} = Z_{21}^{MT} = \frac{(-j\omega L_s + \frac{1}{j\omega C_s}) + j\omega C_p[-\omega^2(L_s^2 - L_m^2) + 2\frac{2(L_s + L_m)}{C_s}]}{1 - 2\omega^2 C_p(L_s + L_m)} \tag{6}$$

$$Y_{11}^{MT} = Y_{22}^{MT} = \frac{j\omega L_s + 1/(j\omega C_s)}{-\omega^2(L_s^2 - L_m^2) + 2(L_s + L_m)/C_s} + j\omega C_p \tag{7}$$

$$Y_{12}^{MT} = Y_{21}^{MT} = \frac{j\omega L_s - 1/(j\omega C_s)}{-\omega^2(L_s^2 - L_m^2) + 2(L_s + L_m)/C_s} - j\omega C_p. \tag{8}$$

To be an equivalent circuit, the modified-T model should have very similar frequency responses to those in a lossless transmission line for both *Z* and *Y* parameters over the entire modeling bandwidth. At low frequencies,

0-7803-7695-1/03/$17.00 © 2003 IEEE

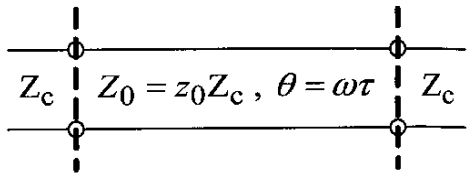

Fig. 2. The transmission-line configuration used for comparing its two-port S parameters with those in a modified-T model. Note that $\tau = 100$ ps for this case.

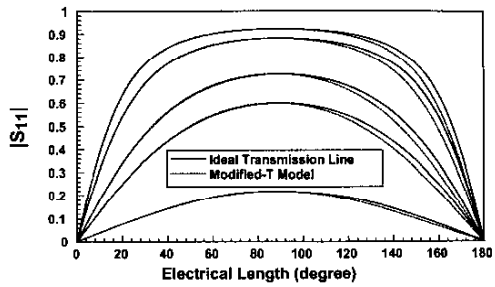

Fig. 3. Comparison of the magnitude of S_{11} versus electrical length between a lossless transmission line and the equivalent modified-T model.

the modified-T model basically reduces to a simple T-section model, and thus two equations based on Z parameters can be established as

$$\lim_{\substack{\theta\to 0\\ \omega\to 0}} \frac{1}{\omega}\left(\frac{1}{Z_{12}^{TL}} - \frac{1}{Z_{12}^{MT}}\right) = 0 \tag{9}$$

$$\lim_{\substack{\theta\to 0\\ \omega\to 0}} \frac{1}{\omega}\left[(Z_{11}^{TL} - Z_{12}^{TL}) - (Z_{11}^{MT} - Z_{12}^{MT})\right] = 0 . \tag{10}$$

From (9) and (10), one can find

$$C_s = \tau / Z_0 \tag{11}$$

$$L_s + L_m = (Z_0\tau)/2 . \tag{12}$$

From (1)-(4) we can know that both Z and Y parameters of an ideal transmission line have a pole at $\theta = \pi$. Thus, we need to create the same pole for the modified-T model by setting the denominators of the corresponding Z and Y parameters in (5)-(8) to zero at the angular half-wave frequency ($\omega_h = \pi/\tau$). That is

$$1 - 2\omega_h^2 C_p (L_s + L_m) = 0 \tag{13}$$

$$-\omega_h^2 (L_s^2 - L_m^2) + 2(L_s + L_m)/C_s = 0 . \tag{14}$$

From (12)-(14), the other three unknown elements in a modified-T model can be found as

$$L_s = Z_0\,\tau\,(1/4 + 1/\pi^2) \tag{15}$$

$$L_m = Z_0\,\tau\,(1/4 - 1/\pi^2) \tag{16}$$

$$C_p = \tau/(Z_0\,\pi^2) . \tag{17}$$

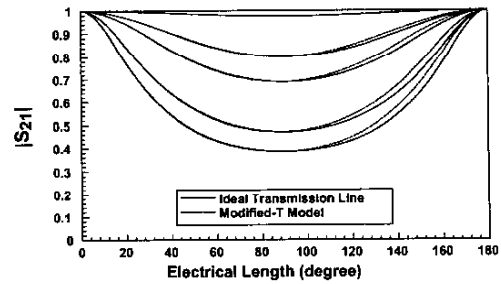

Fig. 4. Comparison of the magnitude of S_{21} versus electrical length between a lossless transmission line and the equivalent modified-T model.

For comparison, we generate the two-port S parameters from the transmission-line configuration shown in Fig. 2, and those from its equivalent modified-T model whose circuit elements have been found using (11) and (15)-(17). As shown in Figs. 3 and 4, comparison of S parameters between transmission lines under various normalized characteristic impedances (z_0) and their equivalent modified-T models shows excellent agreement over an electrical length up to π.

III. Modified-T Model for LTCC Embedded Inductors

The above-mentioned modified-T equivalent circuit can be expanded to model 3-D spiral inductors embedded in a multilayer LTCC substrate, as suggested in Fig. 5. It can be seen that several LC resonators are added to account for the self and ground resonant phenomena. The formulation starts with a derivation of Y network parameters corresponding to the equivalent circuit shown in Fig. 5. Then extraction of equivalent-circuit elements from the measured S parameters can be performed efficiently using the following steps.

Step 1: Formulation with Parallel and Series Resonant Frequencies

First, a new parameter, Y_A, is defined as

$$Y_A \equiv Y_{11} + Y_{22} - 2Y_{12} = \frac{j\omega(L_{s1} + L_{s2} - 2L_m) + 4/Y_{sg}}{-\omega^2(L_{s1}L_{s2} - L_m^2) + j\omega(L_{s1} + L_{s2} + 2L_m)/Y_{sg}} + 4Y_p \tag{18}$$

where

$$Y_{sg} = j\omega C_s b + \left\{ j\omega L_g + [j\omega C_s(1-b)]^{-1} \right\}^{-1} \tag{19}$$

$$Y_p = R_p^{-1} + \left\{ j\omega L_p + (j\omega C_p a)^{-1} \right\}^{-1} + \left\{ j\omega L_{p1} + [j\omega C_p(1-a)]^{-1} \right\}^{-1} . \tag{20}$$

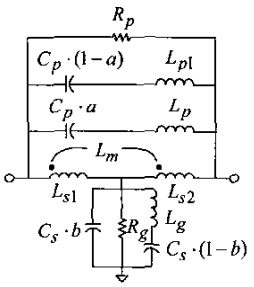

Fig. 5. An expanded modified-T equivalent circuit for modeling an LTCC embedded inductor.

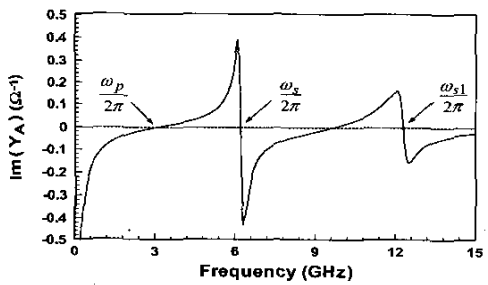

Fig. 6. Determination of parallel and series resonant frequencies from the imaginary part of Y_A.

Assuming $L_{s1} \approx L_{s2}$ and simplifying (18) gives

$$Y_A \approx \frac{4}{j\omega(L_{s1}^{'} + L_{s2}^{'})} + 4Y_p \tag{21}$$

where

$$L_{s1}^{'} = L_{s1} + L_m \tag{22}$$

$$L_{s2}^{'} = L_{s2} + L_m . \tag{23}$$

Fig. 6 shows the imaginary part of Y_A parameter that was found using the measured S parameters for a 6.8 nH spiral inductor embedded in a multilayer LTCC substrate. One root and two poles have been found in this frequency response. The root position represents the parallel resonant frequency ($\omega_p / 2\pi$) while the pole positions represent the first and second series resonant frequencies ($\omega_s / 2\pi$ and $\omega_{s1} / 2\pi$). From the formulations with respect to these three identified frequencies, we can find C_p, L_p, and L_{p1} in the following forms

$$C_p = \left\{ (L_{s1}^{'} + L_{s2}^{'}) \left[a\left(\frac{1}{\omega_p^2} - \frac{1}{\omega_s^2}\right)^{-1} + (1-a)\left(\frac{1}{\omega_p^2} - \frac{1}{\omega_{s1}^2}\right)^{-1} \right] \right\}^{-1} \tag{24}$$

$$L_p = (L_{s1}^{'} + L_{s2}^{'}) \left\{ \left(\frac{\omega_s^2}{\omega_p^2} - 1\right)^{-1} + \frac{1-a}{a}\left(\frac{\omega_s^2}{\omega_p^2} - \frac{\omega_s^2}{\omega_{s1}^2}\right)^{-1} \right\} \tag{25}$$

$$L_{p1} = (L_{s1}^{'} + L_{s2}^{'}) \left\{ \frac{a}{1-a}\left(\frac{\omega_{s1}^2}{\omega_p^2} - \frac{\omega_{s1}^2}{\omega_s^2}\right)^{-1} + \left(\frac{\omega_{s1}^2}{\omega_p^2} - 1\right)^{-1} \right\} . \tag{26}$$

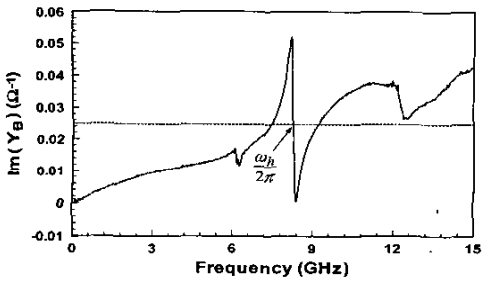

Fig. 7. Determination of half-wave resonant frequency from the imaginary part of Y_B.

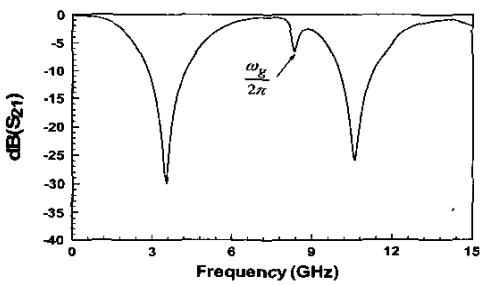

Fig. 8. Determination of ground resonant frequency from the magnitude of S_{21} in decibel.

Step 2: Formulation with Half-Wave and Ground Resonant Frequencies

Another new parameter, Y_B, is defined as

$$Y_B \equiv Y_{11} + Y_{22} + 2Y_{12} = \frac{j\omega(L_{s1} + L_{s2} + 2L_m)}{-\omega^2(L_{s1}L_{s2} - L_m^2) + j\omega(L_{s1} + L_{s2} + 2L_m)/Y_{sg}} . \tag{27}$$

It has been explained before that the denominator of Y parameters for a modified-T model is equal to zero at the half-wave resonant frequency ($\omega_h / 2\pi$). Therefore, it can be practically found from the pole position of the imaginary part of Y_B that was also found from the measured S parameters, as shown in Fig. 7. The finite ground plane effects on an LTCC inductor act as a shunt resonator and usually cause a sudden drop in insertion loss. This can be used to locate the ground resonant frequency ($\omega_g / 2\pi$) quite easily, as shown in Fig. 8. From the formulations with respect to ω_h and ω_g, we can find L_m and L_g in the forms

$$L_m = \frac{L_{s1}^{'} L_{s2}^{'}}{L_{s1}^{'} + L_{s2}^{'}} - \left\{ \omega_h^2 C_s b \left[1 - \frac{(1-b)\omega_g^2}{\omega_h^2 - b\omega_g^2} \right] \right\}^{-1} \tag{28}$$

$$L_g = \frac{1}{\omega_g^2 C_s b (1-b)} . \tag{29}$$

Step 3: Extraction of Fundamental Elements at Low Frequencies and Optimization for Capacitance Split Coefficients

The equivalent-circuit elements in (24)-(29) are all formulated in terms of $L_{s1}^{'}$, $L_{s2}^{'}$, C_s, a and b. At low frequencies, the equivalent circuit shown in Fig. 5 can be approximated as an equivalent T-section model from which we can find the fundamental elements $L_{s1}^{'}$, $L_{s2}^{'}$ and C_s using the following expressions:

$$L_{s1}^{'} = \lim_{\omega \to 0} \frac{\mathrm{Im}\{Z_{11} - Z_{12}\}}{\omega} \tag{30}$$

$$L_{s2}^{'} = \lim_{\omega \to 0} \frac{\mathrm{Im}\{Z_{22} - Z_{12}\}}{\omega} \tag{31}$$

$$C_s = \lim_{\omega \to 0} \frac{\mathrm{Im}\{Z_{12}^{-1}\}}{\omega}. \tag{32}$$

Note that the Z network parameters in (30)-(32) can be obtained from conversion of the measured S parameters. The remaining capacitance split coefficients, a and b, in the formulations can be found quite efficiently using an optimization scheme with the constraints

$$0 \le a \le 1 \tag{33}$$

$$0 \le b \le 1. \tag{34}$$

The parallel and ground resistances, R_p and R_g, are mainly used to account for the losses in the conductor and substrate region respectively. Their values are frequency dependent and can be roughly estimated from the equivalent Π- or T-section models at low frequencies.

A 6.8 nH inductor embedded in a multilayer LTCC substrate was fabricated and measured with S parameters for modeling. The inductor is mainly a 1.5-turn spiral-form conductor with 6-mil width. In Figs. 9 and 10, we compare the S-parameter results generated from our proposed modified-T model and the conventional Π-section model with measurements. It can be seen that the conventional Π-section model is good only up to the parallel resonant frequency that is regarded as the fundamental SRF at about 3 GHz. Our proposed modified-T model can catch not only the parallel resonant frequency, but also the other series and ground resonant frequencies that belong to the higher-order SRFs. The effective bandwidth exceeds 12 GHz, about 4 times larger than the conventional Π-section model.

IV. Conclusions

It is concluded that the proposed modified-T model for LTCC embedded inductors can achieve a bandwidth that is several times larger than the conventional Π-section model. In addition, this model can be constructed quite efficiently because most of the equivalent-circuit elements can be evaluated using the derived analytical expressions.

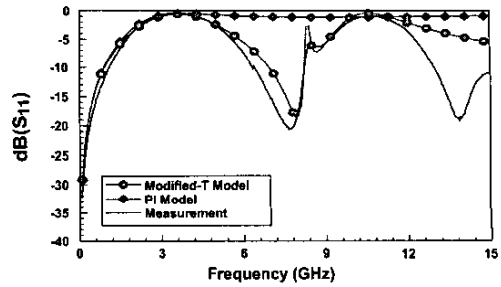

Fig. 9. Comparison of the magnitude of S_{11} in decibel between our proposed modified-T model and the conventional Π-section model with measurements for an LTCC embedded inductor.

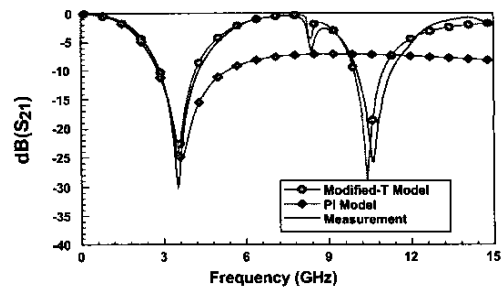

Fig. 10. Comparison of the magnitude of S_{21} in decibel between our proposed modified-T model and the conventional Π-section model with measurements for an LTCC embedded inductor.

V. Acknowledgments

This work was supported by the ROC MOE Program for promoting academic excellence of Universities under the grant number 甲 91-E-FA08-1-4.

References

[1] S. Chaki, S. Aono, N. Andoh, Y. Sasaki, N. Tanino, and O. Ishihara, "Experimental study on spiral inductors," in *IEEE MTT-S Int. Microwave Symp. Dig.*, 1995, pp. 753-756.

[2] M. Rytivaara and F.L. Oy, "Buried passive elements manufactured in LTCC," in *Proc. IEE Seminar on Packaging and Interconnects at Microwave and MM-Wave Frequencies*, 2000, pp. 6/1-6/5.

[3] A. Sutono, D. Heo, Y.E. Chen, and J. Laskar, "High-Q LTCC-based passive library for wireless system-on-package (SOP) module development," *IEEE Trans. Microwave Theory Tech.*, vol. 49, pp. 1715-1724, Oct. 2001.

[4] K.H. Drue, H. Thust, and J. Muller, "RF models of passive LTCC components in the low Gigahertz-range," *Applied Microwave and Wireless*, pp. 26-35, April 1998.

[5] S. Lee, J. Choi, G.S. May, and I. Yun, "Modeling and analysis of 3-D solenoid embedded inductors," *IEEE Trans. Electron. Packag. Manufact.* vol. 25, pp.34-41, 2002.